

# Synthesis, characterization and solid-state properties of [Zn(Hdmmthiol)<sub>2</sub>].2H<sub>2</sub>O complex

Fethi Dagdelen<sup>1,a</sup>, Yildirim Aydogdu<sup>2,b</sup>, Kamalendu Dey<sup>3,c</sup>, and Susobhan Biswas<sup>4,d</sup>

<sup>1</sup> Department of Physics, Faculty of Science, Firat University, Elazig, Turkey

<sup>2</sup> Department of Physics, Faculty of Science, Gazi University, Ankara, Turkey

<sup>3</sup> Department of Chemistry, University of Kalyani, Kalyani 741 235, West Bengal, India

<sup>4</sup> Department of Physics, Jadavpur University, Jadavpur, Kolkata-700032, India

Received: 15 February 2016

Published online: 10 May 2016 – © Società Italiana di Fisica / Springer-Verlag 2016

**Abstract.** The zinc(II) complex with tridentate thiohydrazone ligand have been prepared by metal template reaction. The metal template reaction was used to prepare the zinc (II) complex with tridentate thiohydrazone ligand. The reaction of diacetylmonoxime and, morpholine N-thiohydrazidewith Zn(OAc)<sub>2</sub>.2H<sub>2</sub>O under reflux yielded the formation of the [Zn(Hdmmthiol)<sub>2</sub>].2H<sub>2</sub>O complex. The complex was characterized by a combination of protocols including elemental analysis, UV+vis, FT-IR, TG and PXRD. The temperature dependence of the electrical conductivity and the optical property of the [Zn(Hdmmthiol)<sub>2</sub>].2H<sub>2</sub>O complex is called H<sub>2</sub>dammthiol was studied. Powder X-ray diffraction (PXRD) method was used to investigate the crystal structure of the sample. The zinc complex was shown to be a member of the triclinic system. The zinc complex was determined to have n-type conductivity as demonstrated in the hot probe measurements. The complex was determined to display direct optical transition with band gaps of 2.52 eV as determined by the optical absorption analysis.

## 1 Introduction

A considerable interest has been raised over the past two decades towards the investigation of metal complexes of Schiff bases containing nitrogen and other donors [1–4]. The stability, biological activity [5] or the potential availability of fields of application including the field of catalysis for these bases might be the reason [6]. The metalloprotein's capability for carrying out specific functions depends mainly on its coordination geometry, which determines the environment around the metal center, the number of coordinated ligands and on the donor group [7]. The coordination of metals at the active sites of metallobiomolecules is affected strongly by the nitrogen and sulfur atoms [8]. The variety of ways in which the Schiff base ligands containing various donor atoms such as N, O, and S are bonded to metal ions cause these bases to display broad biological activity and therefore are of special interest. The activity of biologically active compounds may be enhanced by the existence of metal ions that are bonded to them [9–11]. Furthermore the planner structure of complexes of thiohydrazone ligands stabilized by hydrogen bonding may be thought to contribute to their exceptional stability and unique electronic properties [12–14].

The synthesis and the study of molecular complexes, behaving in a similar manner to semiconductors or showing high conductivity has attracted considerable interest. Schottky diodes, solid state devices and optical sensors are among device applications that make use of the potential of semiconducting and optical materials, which manipulate the optical and electrical properties of the metal complexes [15,16]. The elucidation of the electronic structure of these materials may be facilitated through studying the optical absorption of metal complexes, specifically the absorption edge. The optical band gaps could be determined through the analysis of data transmittance and reflectance. The optical absorption spectra allow us to determine the indirect and the direct transitions occurring in the band gap

<sup>a</sup> e-mail: fethidagdelen@gmail.com (corresponding author)

<sup>b</sup> e-mail: yaydogdu@gazi.edu.tr

<sup>c</sup> e-mail: kkey\_chem.@rediffmail.com

<sup>d</sup> e-mail: susobhan\_bis@rediffmail.com

of the metal complexes [8]. One of the most fascinating current research topics is the investigation of the properties of semiconducting metal complexes [17–21]. The remarkable growth of interest in the physics and chemistry of semiconducting metal complexes is reflected by a steady increase in the number of publications.

It is an interdisciplinary field, which combines the interconnected efforts of chemists and physicists. Several studies have recently studied the temperature-dependent electrical properties, thermal conductivity, crystal structure, microstructure and optical properties of novel semiconducting metal complexes displaying typical semi-conductance characteristics [17–23].

Until now, there have been a limited number of studies reporting the electrical, optical and thermal properties of coordination complexes. Recently, there has been a growing interest in such fields that explore some unresolved exciting features of such complexes. The aim of the present investigation is to study the thermal, electrical and optical properties of the  $[\text{Zn}(\text{Hdmmthiol})_2] \cdot 2\text{H}_2\text{O}$  complex.

## 2 Experimental

### 2.1 Materials and methods

The chemicals used were of A.R. grade. The solvents and the chemicals were purified and dried prior to use employing standard procedures. The elemental analyses were carried out using on the Elementar Vario EL III, Carlo Erba 1108 elemental analyzer at the Sophisticated Analytical Instrument Facility, Central Drug Research Institute, Lucknow. The electronic spectra (in water) were recorded using Hitachi 200-20 and Shimadzu UV-2401PC spectrophotometers and the infrared spectra (KBr) were recorded using Perkin-Elmer 1330 and L120-000A FT-IR spectrophotometers. The molar conductance (10 M in water) was measured using an Elico conductivity bridge.

The X-ray powder diffraction data were recorded using a Bruker D8 Advance powder diffractometer using  $\text{Cu K}\alpha$  radiation ( $\lambda = 1.5418 \text{ \AA}$ ). The diffraction pattern was scanned with a step size of  $0.02^\circ$  and a counting time  $7 \text{ s}\cdot\text{step}^{-1}$  over an angular range of  $5^\circ$ – $50^\circ$  ( $2\theta$ ) using the Bragg-Brentano geometry. The X-ray powder diffraction pattern was indexed via the TREOR90 [24] software using the 20 initially observed Bragg reflections. The best solution indicated a triclinic cell with  $a = 10.297368 \text{ \AA}$ ,  $b = 11.325310 \text{ \AA}$ ,  $c = 12.345947 \text{ \AA}$ ,  $\alpha = 111.516869^\circ$ ,  $\beta = 103.288712^\circ$ ,  $\gamma = 91.155464^\circ$  and  $V = 1294.88 \text{ \AA}^3$ .

Approximately 0.1 cm thick tablets of the complex samples were prepared under a pressure of ca.  $1 \times 10^8 \text{ Pa}$  to be utilized in the electrical measurements. Two copper electrodes covered with silver paste were used to test whether the contacts of the prepared tablets were to be Ohmic or not. A two-probe method was used to investigate the electrical conductivities of the complex tablets *via* measuring the current through the probes with a high impedance electrometer (Keithley 6514) upon application of a DC voltage current supplied by an adjustable source of voltage (Keithley 230). A double beam spectrophotometer (Perkin Elmer Lambda 45 Double Beam) was used to measure the optical absorption as a function of the wavelength in the range of 190–1100 nm. The loss in the mass of the sample was determined *via* TG/DTA using a Perkin Elmer Phyris Diamond TG/DTA. The mass loss experiments were carried out under  $\text{N}_2$  atmosphere in a temperature range of 30–580 °C with a heating rate of  $20^\circ\text{C}\cdot\text{min}^{-1}$ .

### 2.2 Synthesis of the $[\text{Zn}(\text{Hdmmthiol})_2] \cdot 2\text{H}_2\text{O}$ complex

The mixture of diacetylmonoxime (0.5 g, 0.005 mol) and morpholine N-thiohydrazide (0.8 g, 0.005 mol) was heated under gentle reflux in the presence of  $\text{Zn}(\text{OAc})_2 \cdot 2\text{H}_2\text{O}$  (0.5475 g, 0.0025 mol) in 50 mL water-methanol (1:1, v/v) mixture. The yellow colored compound thus formed, was recrystallized using chloroform. Yield-5.14 g (60%). *Anal.* Calc. for  $\text{C}_{18}\text{H}_{34}\text{N}_8\text{O}_6\text{S}_2\text{Zn}$ : C, 36.77; H, 5.83; N, 19.06; Zn, 11.12. Determined: C, 36.56; H, 5.89; N, 18.97; Zn 11.03%.  $\Lambda_M$ ,  $13.8 \Omega^{-1} \text{ cm}^2 \cdot \text{mol}^{-1}$ ,  $\lambda_{\text{max}/\text{nm}}$  ( $\epsilon \text{ M}^{-1} \cdot \text{cm}^{-1}$ ): 481(20,225), 228(40,564), 285(45,450), and 207(67,252). IR (KBr pellet)  $\nu_{\text{max}}$  ( $\text{cm}^{-1}$ ) 1608 (C=N, azomethine), 1545(–N=C–S), 756 (C–S), 1027 (N–N), 948 (N–O) and 2990–3264(O–H, oxime).

## 3 Results and discussion

The  $[\text{Zn}(\text{Hdmmthiol})_2] \cdot 2\text{H}_2\text{O}$  complex with tridentate thiohydrazone ligand, diacetylmonoxime morpholine N-thiohydrazone (Hdammmth) was prepared in a metal template reaction. The complex was characterized by means of an elemental analysis, and the utilization of spectroscopic data (infrared, UV-Vis) and X-ray powder diffraction data. The structure of the complex is displayed in fig. 1.

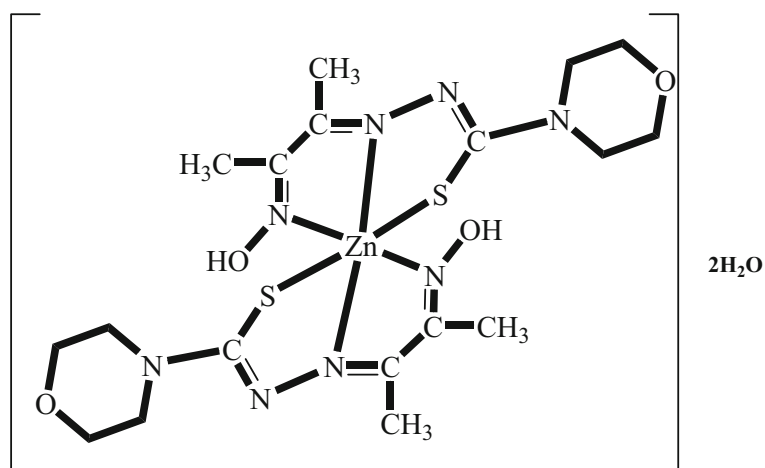


Fig. 1. The structure of the  $[Zn(Hdmmthiol)_2] \cdot 2H_2O$  complex.

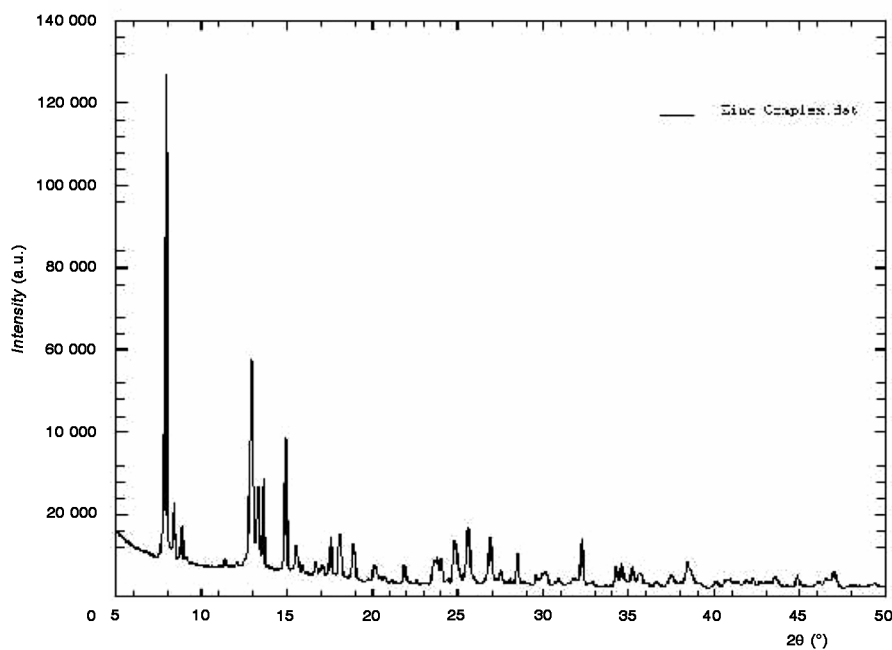


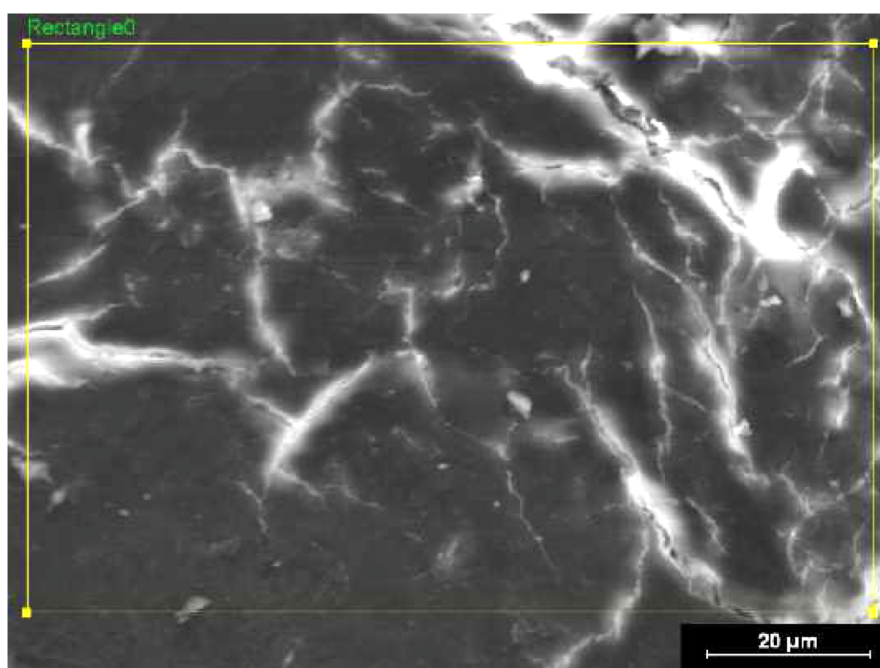
Fig. 2. PXRD pattern of the  $[Zn(Hdmmthiol)_2] \cdot 2H_2O$  complex.

### 3.1 X-ray powder diffraction

X-ray powder diffraction study of the zinc complex was recorded in the analysis and is displayed in fig. 2. The  $d$  values at various diffracting angles ranging from  $7.962^\circ$  to  $32.247^\circ$  are recorded in table 1. The peaks are indexed using the TREOR software [24]. The indexed  $h k l$  values are also provided along with their corresponding  $d$  and  $2\theta$  values in table 1. The results showed that all the complexes belonged to the triclinic system. The corresponding lattice parameters are also provided in table 1. SEM investigation of the ground powders and the fracture surfaces indicated that the grain size distribution was not uniform. We observed submicron grains (finely ground powder) as well as grains even above  $20 \mu m$  (fracture surfaces) (fig. 3). Furthermore, the EDX analyses of the metal complexes indicated the presence of metal along with C and S. The results suggest the formation of metal complexes along with the ligand (Electronic Supplementary Information, fig. 4).

**Table 1.** X-ray Powder diffraction data of the zinc complex.

$a = 10.297368 \text{ \AA}$ , $b = 11.325310 \text{ \AA}$ , $c = 12.345947 \text{ \AA}$ , $\alpha = 111.516869^\circ$ , $\beta = 103.288712^\circ$ , $\gamma = 91.155464^\circ$ , crystal system-triclinic, $V = 1294.88 \text{ \AA}^3$						
$h$	$k$	$l$	$2\theta_{\text{obs}}$	$2\theta_{\text{calc}}$	$D_{\text{obs}}$	$I_{\text{max}}$
0	0	1	7.962	7.955	11.0950	100.0
0	1	0	8.438	8.442	10.4703	7.877
1	0	0	8.894	8.876	9.9352	6.196
1	1	0	12.930	12.951	6.8413	82.991
1	0	1	13.357	13.363	6.6234	25.789
0	1	1	13.645	13.652	6.4843	20.235
0	-1	2	14.937	14.924	5.9262	34.461
-2	0	1	17.559	17.555	5.0467	10.413
1	-2	1	18.117	18.115	4.8925	17.902
1	-1	2	18.913	18.921	4.6885	14.867
-1	-1	3	21.893	21.909	4.0566	8.241
-2	-2	1	23.779	23.771	3.7389	12.822
0	0	3	24.039	24.020	3.6990	12.231
2	1	1	24.815	24.819	3.5851	23.789
-1	-3	1	25.589	25.596	3.4784	28.228
2	0	2	26.900	26.912	3.3117	28.081
0	1	3	28.452	28.456	3.1345	11.471
0	0	4	32.247	32.216	2.7738	18.265

**Fig. 3.** SEM micrograph of the  $[\text{Zn}(\text{Hdmmthiol})_2] \cdot 2\text{H}_2\text{O}$  complex.

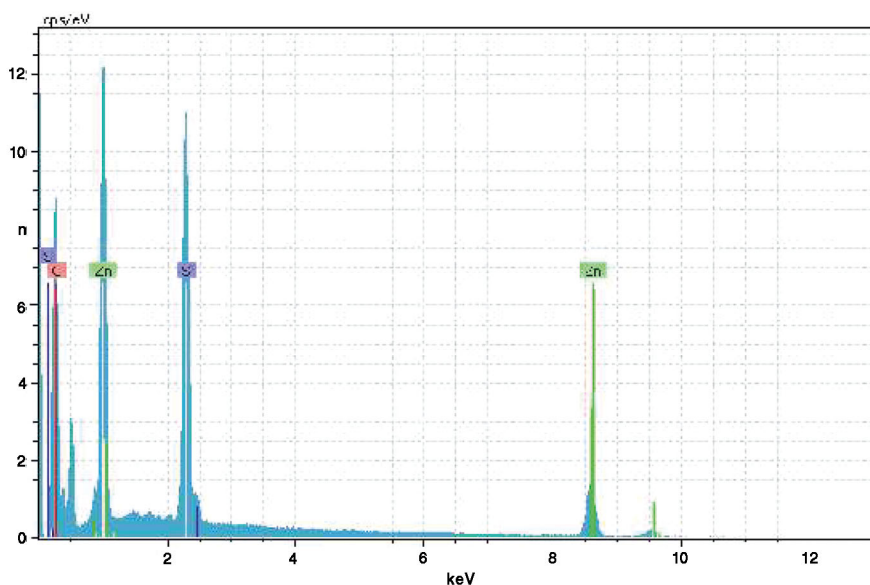


Fig. 4. EDX result of the  $[\text{Zn}(\text{Hdmmthiol})_2] \cdot 2\text{H}_2\text{O}$  complex.

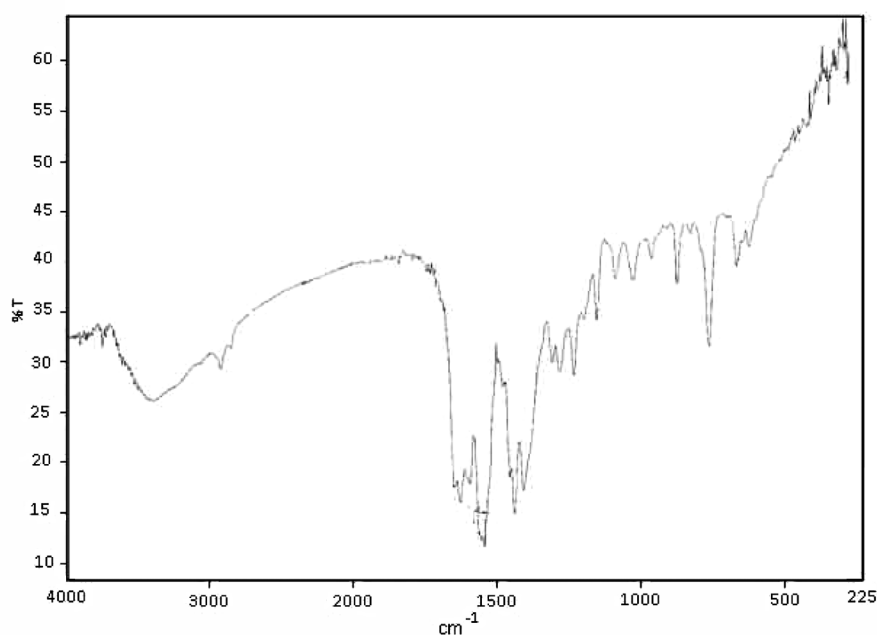


Fig. 5. Infrared spectroscopy of the  $[\text{Zn}(\text{Hdmmthiol})_2] \cdot 2\text{H}_2\text{O}$  complex.

### 3.2 Infrared spectroscopy

The spectra of  $[\text{Zn}(\text{Hdmmthiol})_2] \cdot 2\text{H}_2\text{O}$  displays bands at  $3442 \text{ cm}^{-1}$  for  $\nu(\text{OH})$  (Electronic Supplementary Information, fig. 5). The presence of new bands at  $1608 \text{ cm}^{-1}$  for  $\nu(\text{C}=\text{N})$  of the azomethine group and at  $845 \text{ cm}^{-1}$  for  $\nu(\text{C}-\text{S})$ , suggested the bonding of the thiolate sulfur to the metal ion. The absence of  $\nu(\text{NH})$ , and  $\nu(\text{C}=\text{S})$  bands as well as the appearance of a new band at  $1545 \text{ cm}^{-1}$  characterizing the  $\nu(\text{C}=\text{N})$  of  $-\text{N}=\text{C}-\text{S}$  suggested that the NH protons were lost *via* thioenolization. Furthermore, the presence of a band at ca.  $450\text{--}460 \text{ cm}^{-1}$  was attributed to  $\nu(\text{M}-\text{N})$ . The thioamide band, which contains considerable  $\nu(\text{CS})$  character, was less intense in the complexes and was identified at a lower frequency, suggesting the coordination of the metal through sulfur following deprotonation [25, 26]. Coordination of the thiol S-atom was further designated by the presence of a band at ca.  $360\text{--}380 \text{ cm}^{-1}$  possibly attributed to  $\nu(\text{M}-\text{S})$ .

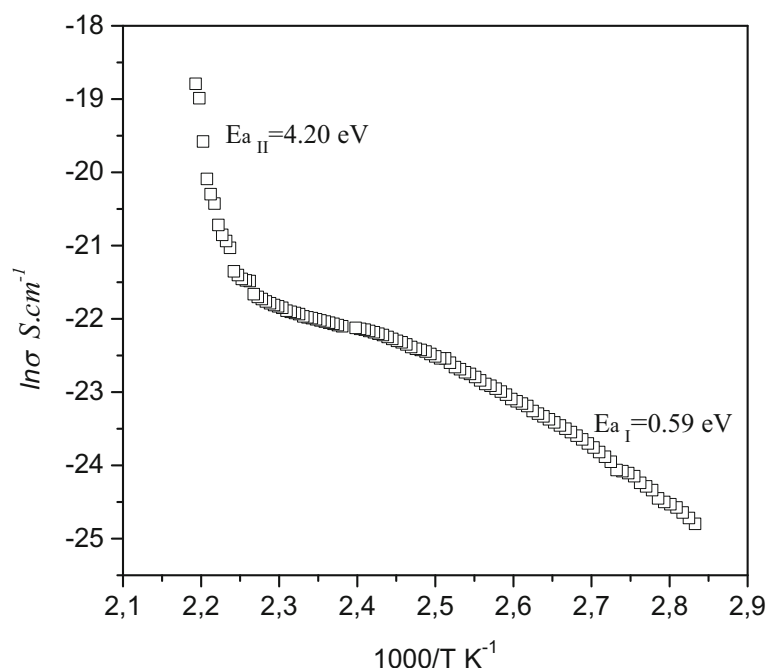


Fig. 6. Temperature dependence on the electrical conductivity of the zinc complex.

### 3.3 Electrical conductivity of the zinc complex

The variation in the electrical conductivity of the zinc complex in response to the reciprocal of the absolute temperature was displayed in fig. 6 in a logarithmic scale. Equation (1) relates the electrical conductivity of a semiconductor material dependent on temperature [27]:

$$\sigma = \sigma_0 \exp(-E_a/kT), \quad (1)$$

with  $\sigma_0$ ,  $E_a$  and  $k$  being the pre-exponential factor, the energy of activation and the Boltzmann constant, respectively. This relation is used to calculate the energy of activation. The thermal energy of activation of the zinc complex was thus determined from the linear slope of the plot of  $\log \sigma$  vs.  $1000/T$ . It was observed that the complex exhibited different behavior in two distinct regions, depending on the temperature and therefore the complex was determined to have two different energies of activation. At low temperatures (350–425 K) (large  $1/T$ ) the extrinsic behavior was observed to dominate. The energy of activation for the complex was calculated to be low (0.59 eV) in the lower temperature range (350–425 K), whereas it was significantly higher (4.20 eV) in the high-temperature range (425–455 K). Furthermore, the transition region denoted the region of saturation and the carrier density was not greatly influenced by temperature in this region.

The conductivity of the compound displayed the typical Arrhenius-type dependence on temperature. The mechanism of such an  $n$ -type electrical semiconductivity of the present Schiff base complexes could be explained in view of the transfer of electrons in two different possible ways. One of the possible mechanisms suggested that, the conduction process could be assumed to have begun with the delocalization of the  $p$ -electrons followed by the excitation of electrons from HOMO to LUMO of the  $p$ -MOs, which was indeed reported to convert metal complexes to their semiconducting state [28,29]. The other possible mechanism suggested that, the electrons hopped from one localized metal site to the next and this explanation presumed that, the gaps had little effect on the mobility of the negative charges. Thus, the electrons were thought to act as passageways from one molecular unit to the similar vacant level of the neighboring molecular unit. In this case the tunneling of the electrons through the intermolecular potential barrier was observed to occupy the corresponding orbital in the contiguous unit via  $p$ - $p$  stacking and extensive H-bonding.

### 3.4 Optical properties

The optical absorption measurement was recorded over the wavelength range of 400–1100 nm. The dependence of the crystalline and amorphous materials on optical absorption is expressed by the following relationship [27,30]:

$$(\alpha h\nu)^2 = A(h\nu - E_{gd}), \quad (2)$$

where  $\alpha$  is the absorption coefficient,  $A$  is a constant,  $E_{gd}$  is the optical band gap,  $h\nu$  is the photon energy.

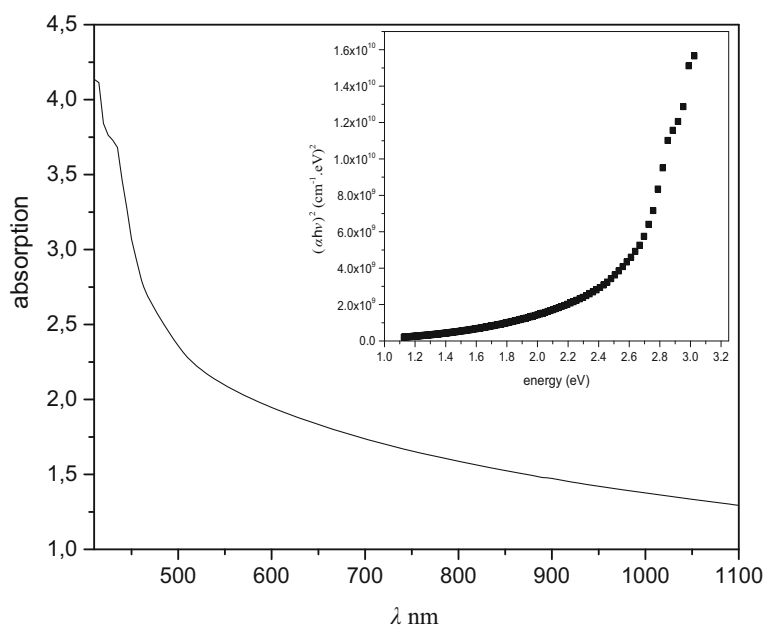


Fig. 7. The optical absorption spectra for complex.

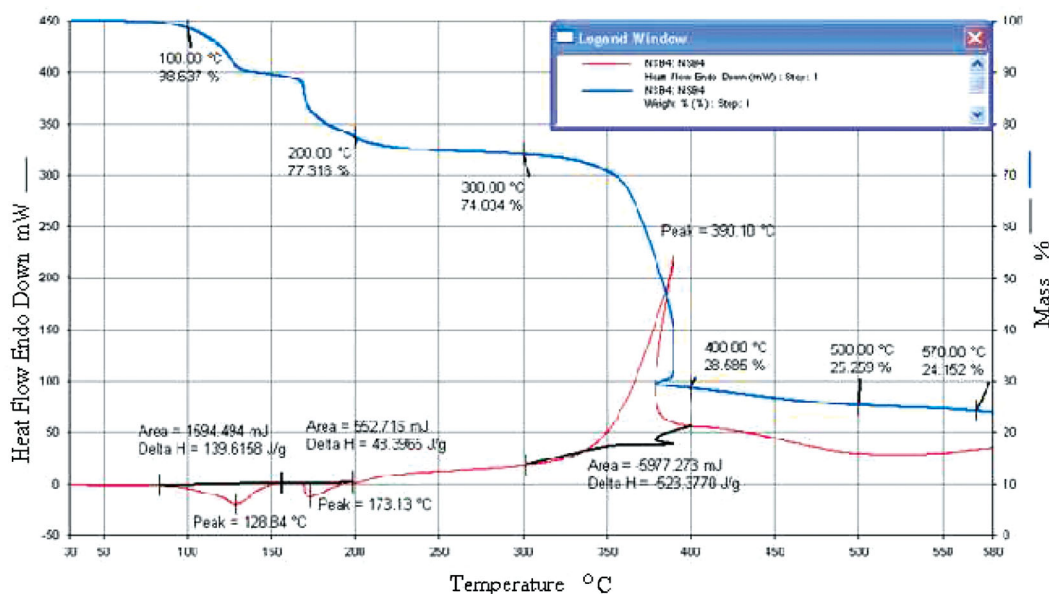


Fig. 8. TG/DTA curves of the  $[Zn(Hdmmthiol)_2] \cdot 2H_2O$  complex.

A plot of  $(\alpha h\nu)^2$  versus  $h\nu$  is shown in fig. 7. The direct band gap value was calculated from the extrapolation of the linear range of the plot, which was parallel to the energy axis. The predominant optical transition of  $h\nu$  was determined by analyzing the absorption data and a direct gap was observed to exist. The optical band gap  $E_{gd}$  was obtained by the plot of  $(\alpha h\nu)^2 = 0$ . Least square fitting was used on the data points in order to obtain the value of the optical band gap  $E_{gd}$  and this value was determined at room temperature as 2.52 eV for the zinc complex.

### 3.5 Thermal properties

The thermal decomposition of the Zn(II) complex measured in a temperature range starting from room temperature up to 580 °C displayed three stages of decomposition as shown in fig. 8. For the complex under investigation, the first stage of decomposition commenced at around 100 °C and was complete at ca. 150 °C. This stage was responsible for approximately, 10% of the total mass loss. This corresponds to the expulsion of the  $H_2O$  group from the Zn(II) complex. The second clearly distinguishable stage of decomposition was observed in the range of ca. 170–200 °C and the loss

in mass was determined as 13%. The second stage of mass loss corresponds to the elimination of the thiohydrazone ligand. The last stage of decomposition commenced at about a temperature range of 300–400 °C and, approximately 45% of the mass was lost during this stage. This decomposition step (> 300 °C) characterized the composition of ZnS in the complex.

The DTA peaks correlated well with the TG curves. The two endothermic peaks were observed at the temperature ranges of ca. 100–150 °C and ca. 170–200 °C, which correspond to the two initial stages of decomposition. The third peak was determined to be exothermic peak and it was observed in an approximate temperature range of ca. 300–400 °C.

## 4 Conclusion

Schottky diodes, solid-state devices and optical sensors are among device applications that make use of the potential of semiconducting and optical materials, which manipulate the optical and electrical properties of the metal complexes and therefore such research has gained increased impact. The major carriers of the zinc complex under investigation were determined to be the electrons via the electrical measurements that were conducted. Therefore *n*-type semiconductance properties could be attributed to the complex. The zinc complex was determined to have a 2.52 eV direct band gap. Applications involving semi-conducting and optical devices constructed using materials made from this zinc complex would benefit extensively from a thorough understanding of the electrical and optical properties of this complex.

We acknowledge the Sophisticated Instrumentation Facility, Central Drug Research Institute, Lucknow, India for carrying out the elemental analysis and providing the spectroscopic data. Facilities provided by the DST, Govt. of India, New Delhi under FIST grant to Dept. of Chemistry, Kalyani University are also gratefully acknowledged.

## References

1. S.S. Djbbbar, B.O. Benali, J.P. Deloume, *Polyhedron* **16**, 2175 (1997).
2. P. Bhattacharya, J. Parr, A.T. Ross, A.M.Z. Slawin, *J. Chem. Soc. Dalton Trans.* **19**, 3149 (1998).
3. L. He, S.H. Gou, Q.F. Shi, *J. Chem. Crystallogr.* **29**, 207 (1999).
4. J.C. Wu, N. Tang, W.S. Liu, M.Y. Tan, A.C.S. Chan, *Chin. Chem. Lett.* **12**, 757 (2001).
5. C.M. Liu, R.G. Xiong, X.Z. You, Y.J. Liu, K.K. Cheung, *Polyhedron* **15**, 4565 (1996).
6. A. Galdes, B.L. Vallee, *Zinc and its Role in Biology and Nutrition*, edited by H. Sigel (Marcel Dekker, New York, 1983).
7. R. Klement, F. Stock, H. Elias, H. Paulus, P. Pelikan, M. Valko, M. Mazur, *Polyhedron* **18**, 3041 (1999).
8. K.D. Karlin, J. Zubieta, *Biological and Inorganic Copper Chemistry* (Adenine Press, New York, 1983).
9. G.G. Mohamed, *Spectrochim. Acta A* **64**, 188 (2006).
10. L. Shi, W.J. Mao, Y. Yang, H.L. Zhu, *J. Coord. Chem.* **62**, 3471 (2009).
11. M.A. Phaniband, S.D. Dhumwad, *Trans. Met. Chem.* **32**, 1117 (2007).
12. S. Biswas, S. Sarkar, I.M. Steele, G. Mostafa, B.B. Bhaumik, K. Dey, *Polyhedron* **26**, 5061 (2007).
13. S. Biswas, G. Mostafa, I.M. Steele, S. Sarkar, K. Dey, *Polyhedron* **28**, 1010 (2009).
14. S. Biswas, G.P.A. Yap, K. Dey, *Polyhedron* **28**, 3094 (2009).
15. F. Dagdelen, A. Aydogdu, *Sci. Eng. J. Firat. Univ.* **18**, 291 (2006).
16. Y.S. Ocak, M.A. Ebeoglu, G. Topal, T. Kılıçoglu, *Physica B* **405**, 2329 (2010).
17. S. Sarkar, Y. Aydogdu, F. Dagdelen, B.B. Bhaumik, K. Dey, *Mater. Chem. Phys.* **88**, 357 (2004).
18. W.J. Liu, G.X. Xiong, W.P. Wang, *Appl. Organometall. Chem.* **21**, 83 (2007).
19. J.D. Chellain, J. Johnson, *Spectrochim. Acta Part A* **127**, 396 (2014).
20. S. Biswas, F. Dagdelen, Y. Aydogdu, K. Dey, *Mater. Chem. Phys.* **129**, 1121 (2011).
21. F. Dagdelen, *Investigation of the Electronic Properties of Metal-Complex Semiconductor Schottky Diodes*, Firat University, PhD Thesis (2004).
22. R.S. Joseyphus, E. Viswanathan, C.J. Dhanaraj, J. Joseph, *J. King Saud Univ. Sci.* **24**, 233 (2012).
23. N. Singh, S. Gupta, *Synth. Metals* **110**, 207 (2000).
24. P.E. Werner, L. Eriksson, M. Westdahl, *J. Appl. Cryst.* **18**, 367 (1985).
25. S. Sarkar, S. Biswas, K. Dey, B.B. Bhaumik, *J. Coord. Chem.* **60**, 1057 (2007).
26. M.A. Ali, R.N. Bose, *Polyhedron* **3**, 517 (1984).
27. F. Gutmann, *Organic Semiconductors* (Wiley, New York, 1967).
28. G.B. El-Hefnawey, M.M. Ayad, A.E. El-Trass, *Thermochim. Acta* **198**, 345 (1992).
29. K.Y. El-Baradie, M. Gaber, M.M. Abou-Sekkina, *Thermochim. Acta* **246**, 175 (1994).
30. J.I. Pankove, *Optical Processes in Semiconductors* (Prentice-Hall Inc, New Jersey, 1971).